SiliconPV 2023, 13th International Conference on Crystalline Silicon Photovoltaics
Carrier Selective Contacts, Metallization and Contact Formation
https://doi.org/10.52825/siliconpv.v1i.877

Published: 22 Feb. 2024

Key Aspects of *p*-Type TOPCon on Textured Surface for Silicon Bottom Cells in Tandem Devices

Jana-Isabelle Polzin[1][https://orcid.org/0000-0002-2372-164X], Katrin Krieg[1], Armin Richter[1][https://orcid.org/0000-0002-7232-8385], Sven Kluska[1][https://orcid.org/0000-0001-9054-2636], Jan Benick[1][https://orcid.org/0000-0002-9433-1171], and Martin Hermle[1][https://orcid.org/0000-0002-2412-1734]

[1] Fraunhofer-Institute for Solar Energy Systems ISE, Germany

Abstract. Both-sides TOPCon solar cells are an interesting candidate for a highly efficient and thermally robust Silicon (Si) bottom cell for tandem devices, such as Perovskite-Si solar cells. However, preparation of *p*-type TOPCon on a textured surface is necessary which is particularly challenging. This work aims to gain a deeper understanding of the limiting factors and thereby optimize the SiO_x/poly-Si(p) contact to close the gap to its *n*-type counterpart. Using symmetrical lifetime samples, we first show that a high level of surface passivation can be achieved using thermally grown interfacial oxides of different thicknesses. The samples strongly benefit from an effective thermal activation of hydrogenation by means of fast-firing. Thus, a recombination current density J_{0s} as low as 23.4 fA/cm² was achieved for *p*-type TOPCon on textured surface featuring an *in situ* Boron-doped poly-Si layer prepared by plasma enhanced chemical vapor deposition (PECVD). Moreover, we show that the passivation quality strongly depends on surface morphology. Smoothening the random pyramids' valleys and – what is more – the tips has a positive impact on the surface passivation.

Keywords: Silicon Bottom Cells, TOPCon, In Situ Boron-Doped Poly-Si

1. Introduction

The efficiencies of crystalline Si solar cells in both research and development as well as industry steadily approach the theoretical limit of 29.4 %. Perovskite-Si tandem solar cells are a promising approach to further increase the efficiency potential. Currently, Silicon heterojunction (SHJ) technology is dominating in the application as a Si bottom cell. However, cells featuring *n*- and *p*-type poly-Si based passivating contacts (TOPCon) at the front and rear, so called TOPCon² cells, seem to be an appealing alternative due to their enhanced thermal stability as well as improved cost-effectiveness [1]. For an excellent infrared response, a textured surface at the rear is indispensable. However, the realization of *p*-type TOPCon on textured surface morphology is particularly challenging due to a higher interface state density D_{it} – and thus recombination current density J_0 [2] – as well as a decreased SiO_x growth rate on (111)- compared to (100)-oriented surfaces found on the pyramids' planes resulting in a nonuniformity in oxide growth across the wafer surface [3]. The latter is more relevant for *p*-type compared to *n*-type TOPCon as Boron (B) readily passes the poly-Si/ SiO_x interface [4] and penetrates the oxide [5].

In this paper, we first address the influence of the interfacial oxide and thermal activation of hydrogenation on the surface passivation of *p*-type TOPCon prepared on textured surfaces. Furthermore, we investigate different approaches to alter the morphology of random pyramids' tips or valleys and show the impact on the passivation quality as well as optical properties.

2. Effective Surface Passivation

2.1 Experimental Layout

Firstly, we investigated different approaches with regards to their effectiveness to improve the surface passivation of *p*-type TOPCon by means of symmetrical test structures. To this end, two interfacial oxides SiO_x of different thicknesses were thermally grown on alkaline textured float zone wafers (4-inch n-type 3 Ωcm, 200 µm thick). The thin SiO_x was measured to 1.3 nm, the thick SiO_x 2.7 nm which were then capped with 50 nm of *in situ* B-doped poly-Si prepared by PECVD. B_2H_6 served as doping gas. High-temperature annealing was performed at T_{anneal} = 950°C or 1000°C for 10 min in N_2 atmosphere and a 70 nm thick SiN_x layer was applied as hydrogen source. The samples were then fired using a VCSEL laser system [6]. The effective charge carrier lifetime was assessed using photoconductance decay measurements (Sinton WCT-120) and the surface saturation current density J_{0s} was extracted following [7] using Auger parametrisation by Niewelt *et al.* [8]. Uncertainties of J_{0s} are calculated by error propagation from uncertainties of input parameters and models and are represented by error bars. The contact resistivity across the poly-Si/SiO_x/c-Si junction was measured using vertical I-V measurements.

2.2 Experimental Results

Figure 1 shows J_{0s} of *p*-type TOPCon after annealing, SiN_x deposition and subsequent exposure to fast-firing processes with 750°C or 800°C peak temperature (actual wafer temperature) for the two different SiO_x.

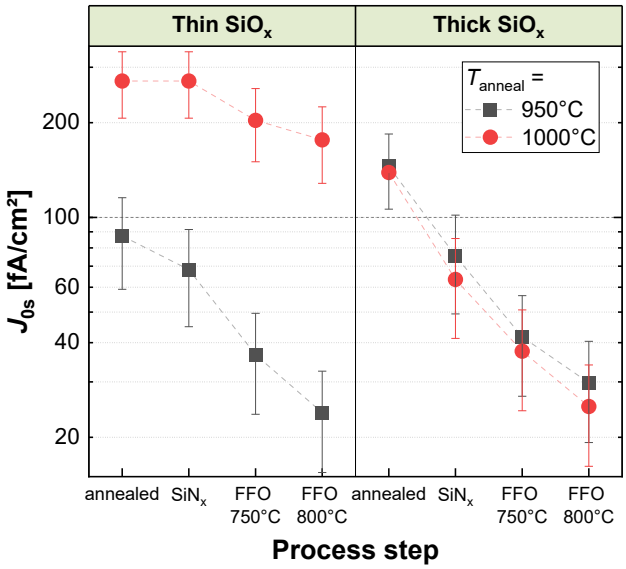

Figure 1. J_{0s} of symmetric *p*-type TOPCon structures determined after different process steps. They feature a 1.3 nm thin or 2.7 nm thick SiO_x and high-temperature annealing was performed at 950°C or 1000°C, respectively.

p-type TOPCon with thin SiO_x on textured surface reached J_{0s} = 87.3 fA/cm² after annealing at 950°C. After SiN_x deposition, the passivation improved slightly, but a subsequent fast-firing step at 800°C reduced J_{0s} significantly to 23.4 fA/cm². When annealed at a higher T_{anneal} = 1000°C, J_{0s} was considerably higher for all process steps. This can be ascribed to enhanced Auger recombination resulting from excessive B diffusion through SiO_x into the c-Si bulk (data not shown here) and presumably breaking up of the oxide layer. With the thick SiO_x, however, J_{0s} was in the range of 139 – 145 fA/cm² after annealing at 950 and 1000°C and thus higher compared to samples with the thinner SiO_x. This might result from a lower field-effect

passivation, but a more intact SiO_x layer compared to the thinner SiO_x at the respective T_{anneal}. Nonetheless, the passivation quality also increased and J_{0s} values of 25.1 or 29.8 fA/cm² after hydrogenation and activation were reached. Noteworthy, this behavior differs from our *n*-type TOPCon samples whose passivation is already fully active after SiN_x deposition. Furthermore, a low contact resistivity ρ_c of approx. 10 mΩcm² was determined for samples with thin SiO_x after annealing at T_{anneal} = 950°C. But with thicker SiO_x, ρ_c > 1,000 mΩcm² even at T_{anneal} = 1000°C and thus this interfacial oxide would not be suitable for implementation into solar cells.

Quokka3 simulations exhibit a V_{oc} potential of 718.6 mV for a TOPCon² bottom cell (or 702.3 mV with 50 % transmission through a tandem top cell) featuring *n*-type TOPCon at the planar front side (J_{0s} = 1 fA/cm²) and *p*-type TOPCon at the textured rear side (J_{0s} = 23.4 fA/cm²).

3. Influence of Surface Morphology

3.1 Experimental Layout

To further understand the correlation between the *p*-type TOPCon passivation quality and surface morphology, alkaline textured wafers (1 Ωcm, p-type FZ, 250 µm thick) received a thermal or wet-chemical post treatment before TOPCon preparation. They were either oxidized at 1050°C or etched in a HF/O_3 mixture for different durations. The samples were then symmetrically coated with a 1.7 nm thin interfacial oxide and 50 nm of *in situ* B-doped a-Si as described above. After annealing at 1000°C, a SiN_x layer was applied as hydrogen source.

3.2 Experimental Results

The SEM images in Figure 2 a) – c) show the textured wafer surface after TOPCon preparation. While Figure 2 a) depicts the standard alkaline textured surface morphology, Figure 2 b) and c) demonstrate that thermal oxidation results in rounding of the pyramids' valleys whereas wet-chemical etching smoothens the pyramids' tips.

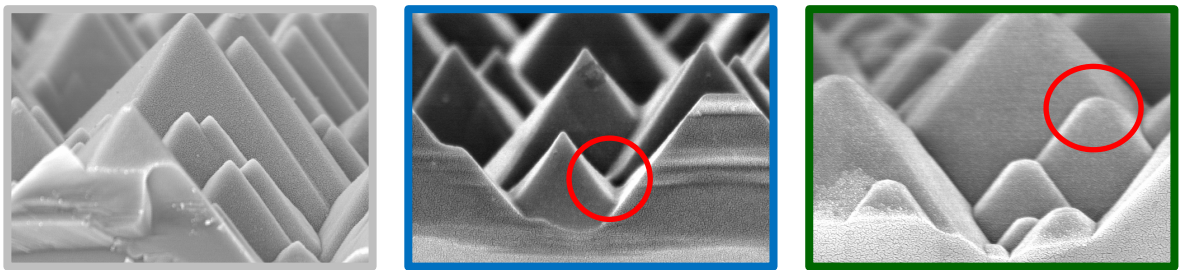

a) b) c)

Figure 2. SEM images of *p*-type TOPCon on a) standard alkaline textured surface and b) long thermal oxidation or c) long wet-chemical etching after texturing and prior to TOPCon preparation.

The influence of the surface morphology on the passivation quality of *p*-type TOPCon is illustrated in Figure 3. It shows the single-sided, area-corrected J_{0s} after SiN_x deposition, prior to fast-firing (taking different area-enlargement factors into account). When prepared on standard alkaline textured surface, J_{0s} took a value of 34.6 fA/cm². Rounding of the pyramids' valleys by thermal oxidation slightly improved the passivation quality to J_{0s} = 32.4 fA/cm² and further to 31.7 fA/cm² with a longer oxidation time. A stronger impact was found for wet-chemically smoothening the pyramids' tips. With increasing etch time, J_{0s} was gradually decreased to 25.4 fA/cm². Thus, the values approach that of the planar reference sample (J_{0s} = 6.6 fA/cm)

but there is still a gap that needs to be addressed by a sufficient hydrogen passivation as pointed out above.

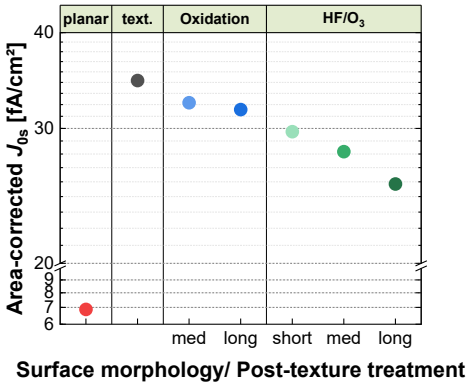

Figure 3. Area-corrected J_{0s} after SiN_x deposition of *p*-type TOPCon prepared on planar and alkaline textured surface including thermal or wet-chemical post-texture treatment.

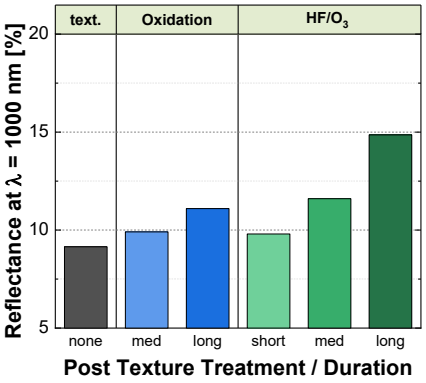

Figure 4. Reflectance of symmetrically textured and differently post texture treated *p*-type TOPCon lifetime samples (without SiN_x capping).

Altering the pyramids' shape is not only beneficial for the passivation but also influences the optical properties. The reflectance was determined in the wavelength range of 300 to 1200 nm. Figure 4 shows the reflectance at a selected wavelength of λ = 1000 nm which is interesting for rear side application of the layer in a solar cell. The surface treatments reduce the antireflection effect of the pyramids. This applies for λ < 1100 nm. As the test samples are both-sides textured, it is not straightforward to determine the impact on the light trapping behavior. Therefore, the next step will be to implement the different post texture treatments into bottom cells processing.

4. Conclusion

In summary, we showed that a high level of surface passivation can be achieved using thermally grown interfacial oxides of different thicknesses. The samples strongly benefit from an effective thermal activation of hydrogenation by means of fast-firing. Eventually, J_{0s} as low as 23.4 fA/cm² was achieved for *p*-type TOPCon on textured surface featuring *in situ* B-doped poly-Si. Moreover, we showed that the passivation quality strongly depends on surface morphology. Smoothening the random pyramids' valleys and especially the tips has a positive impact on the surface passivation.

Data availability statement

The data supporting the results of this contribution are available upon reasonable request from the corresponding author

Author contributions

Jana-Isabelle Polzin: Conceptualization, Data curation, Investigation, Visualization, Roles/Writing – original draft. Katrin Krieg: Resources. Armin Richter: Resources. Jan Benick: Writing – review & editing. Martin Hermle: Funding acquisition, Supervision, Writing – review & editing.

Competing interests

The authors declare no competing interests.

Funding

This work was supported by the German Federal Ministry for Economic Affairs and Climate Action BMWK within the research project “RIESEN” under contract no. 03EE1132A as well as and the Scientific and Technological Research Council of Türkiye (TÜBITAK) under grant number 20AG002 TÜBITAK “SUPERTOP”.

Acknowledgement

The authors would like to thank A. Leimenstoll, F. Schätzle, D. Ourinson, I. Koc for sample preparation and characterization.

References

1. C. Messmer, B. S. Goraya, S. Nold, P. S. Schulze, V. Sittinger, J. Schön, J. C. Goldschmidt, M. Bivour, S. W. Glunz, and M. Hermle, Prog Photovolt Res Appl **29**, 744 (2021). DOI: https://doi.org/10.1002/pip.3372.
2. Y. Larionova, H. Schulte-Huxel, B. Min, S. Schäfer, T. Kluge, H. Mehlich, R. Brendel, and R. Peibst, Sol. RRL **4**, 2000177 (2020). DOI: https://doi.org/10.1002/solr.202000177.
3. A. S. Kale, W. Nemeth, H. Guthrey, S. U. Nanayakkara, V. LaSalvia, S. Theingi, D. Findley, M. Page, M. Al-Jassim, D. L. Young, P. Stradins, and S. Agarwal, ACS applied materials & interfaces **11**, 42021 (2019). DOI: https://doi.org/10.1021/acsami.9b11889.
4. F. Feldmann, J. Schön, J. Niess, W. Lerch, and M. Hermle, Solar Energy Materials and Solar Cells **200**, 109978 (2019). DOI: https://doi.org/10.1016/j.solmat.2019.109978.
5. K. Inoue, F. Yano, A. Nishida, H. Takamizawa, T. Tsunomura, Y. Nagai, and M. Hasegawa, Appl. Phys. Lett. **95**, 43502 (2009). DOI: https://doi.org/10.1063/1.3186788.
6. D. Ourinson, G. Emanuel, K. Rahmanpour, F. Ogiewa, H. Muller, E. Krassowski, H. Hoffler, F. Clement, and S. W. Glunz, IEEE J. Photovoltaics **11**, 282 (2021). DOI: https://doi.org/10.1109/jphotov.2020.3043856.
7. A. Kimmerle, J. Greulich, and A. Wolf, Solar Energy Materials and Solar Cells **142**, 116 (2015). DOI: https://doi.org/10.1016/j.solmat.2015.06.043.
8. T. Niewelt, B. Steinhauser, A. Richter, B. Veith-Wolf, A. Fell, B. Hammann, N. E. Grant, L. Black, J. Tan, A. Youssef, J. D. Murphy, J. Schmidt, M. C. Schubert, and S. W. Glunz, Solar Energy Materials and Solar Cells **235**, 111467 (2022). DOI: https://doi.org/10.1016/j.solmat.2021.111467.